Energy & Environmental Science

Cite this: *Energy Environ. Sci.*, 2011, **4**, 4668

www.rsc.org/ees

PAPER

Mesoporous carbon nitride–silica composites by a combined sol–gel/thermal condensation approach and their application as photocatalysts†

Kamalakannan Kailasam,[a] Jan Dirk Epping,[a] Arne Thomas,*[a] Sebastian Losse[b] and Henrik Junge[b]

Received 18th July 2011, Accepted 31st August 2011
DOI: 10.1039/c1ee02165f

Mesoporous carbon nitrides, silicas and their composites have been prepared by a combined sol–gel and thermal condensation approach. Precursors for the carbon nitride (cyanamide) and silica (TEOS) are mixed and condensed simultaneously. After condensation and heat treatment it is observed that the carbon nitride and silica formed highly interpenetrating mesophases which leads either to the formation of mesoporous carbon nitride or silica after selective removal of one of the phases. Importantly, the carbon nitride preserves its graphitic stacking even in the spatial confinement introduced by the surrounding silica phase. As both precursors are liquids this approach allows convenient shaping into thin and thick films or monoliths of mesoporous carbon nitrides. Enhanced photocatalytic activity is observed for the production of hydrogen from water when these mesoporous carbon nitrides are applied as photocatalyst in comparison to the bulk, but also to other mesoporous carbon nitrides, prepared by the reported two-step, hard templating approach.

Introduction

Carbon nitrides (CNs) are prepared by the pyrolysis of nitrogen-rich precursors. When cyanamide, dicyanamide or melamine is used as a precursor, sheets of ordered tri-*s*-triazine units connected through planar secondary or tertiary amino groups are formed.[1–3] Depending on the degree of condensation the resulting materials are called melon (linear polymers of connected tri-*s*-triazines *via* secondary nitrogen) or graphitic carbon nitrides ($g\text{-}C_3N_4$, 2D sheets of tri-*s*-triazine connected *via* tertiary amines).[4,5] It has been shown that the degree of condensation influences the properties of the materials important for their applications as catalysts[2,6] and photocatalysts.[7–10]

Furthermore it has been shown that the introduction of porosity and high surface area can enhance the catalytic performance of the carbon nitrides to a large extent. The most efficient pathways to create porosity so far are hard templating approaches, extensively described for the preparation of porous carbons or polymers.[11,12] Silica nanoparticles or mesoporous silicas can be used as hard templates to create porous carbon nitrides with ordered or disordered pore structures.[6,9,10,13–17]

Mesoporous carbon nitrides with high surface area and spherical pores of 12 nm arranged in non-regular fashion were for example prepared using silica nanoparticles as templates.[6] Ordered mesoporous carbon nitride with 2D hexagonal pore structure with relatively large mesochannels (10.7 nm) has been

[a]*Institut für Chemie, Sekr. TC 2, Technische Universität Berlin, Englische Str. 20, 10587 Berlin, Germany. E-mail: arne.thomas@tu-berlin.de*
[b]*Leibniz-Institut für Katalyse e. V. an der Universität Rostock, Albert-Einstein-Straße 29a, 18059 Rostock, Germany*

† Electronic supplementary information (ESI) available: Elemental analyses of the carbon nitride materials, TGA curves, nitrogen sorption isotherms and pore size distribution of the carbon nitride–silica composites, and photocatalytic hydrogen production monitored by automatic gas burettes. See DOI: 10.1039/c1ee02165f

Broader context

Converting solar energy into the storable chemical energy of hydrogen by photocatalytic water splitting is of major interest for a future sustainable energy supply. A variety of semiconducting materials has been proposed as more or less efficient photocatalysts for this reaction. Beside the chemical composition, which in the first place determines that the material has a suitable band structure for the splitting of water, it has been shown that the introduction of a nanometre sized structure can have crucial influence on the photocatalytic activity. For example the accompanied increase in the surface area increases the number of catalytically active sites for the splitting of water. The same is true for a so-called graphitic carbon nitride, a metal free, polymeric semiconductor, which has been reasonably shown to be a cheap and abundant alternative as water splitting photocatalyst. The initially low activity of the bulk material could be considerably enhanced by introduction of small pores into this material. In this work we introduce a facile synthesis of mesoporous carbon nitrides, which yield a material with further increased photocatalytic activity.

reported using SBA-15 as template.[17] Also, cubic porous structures were introduced using the respective mesoporous silicas (*e.g.* KIT-6).[18] Surfactants and amphiphilic block copolymers have been used extensively to create mesoporous inorganic materials and have been recently also applied to form porous carbon nitrides, however yielding unordered carbon-incorporated carbon nitrides.[13]

Recently carbon nitride has been introduced as photocatalyst for the production of hydrogen from water.[7] It has been shown that hydrogen evolution is increased by a factor of up to 10 when mesoporous carbon nitrides are applied instead of the bulk material.[9,10] It can thus be concluded that the introduction of porosity into these materials can be crucial to enhance their performance.

Using the described synthetic pathways towards mesostructured carbon nitrides the materials can however be prepared as powders only. Even though cyanamide is a liquid and dicyanamide and melamine could in principle be processed from solution the formation of carbon nitride films or monolith from these precursors is hindered by the sublimation of melamine, which occurs at 335 °C. Still, to expand the application of porous carbon nitrides in the field of catalysis, electrocatalysis, optoelectronics, sensors, separations and others, it would be beneficial, if not mandatory, to synthesize porous materials in the form of thin films or monoliths. Earlier attempts to prepare carbon nitride materials thin films by vapor deposition and nanocasting methods failed due to the elimination of vast majority of N_2, which results in disordered amorphous carbon-rich materials.[15,19–21] Hence novel procedures should be introduced to prepare defined nanostructured carbon nitride materials.

In this study, a facile sol–gel route is employed to synthesize mesoporous carbon nitride, or alternatively mesoporous silicas, by simply mixing their respective precursors, cyanamide and TEOS. Evaporation of the solvent yields silica/cyanamide composite gels, which after heating form silica/carbon nitride biphasic composites. Removal of one of the phases *i.e.* either carbon nitride or silica results in a porous material of the other phase. Through the sol–gel type approach the precursors and subsequently the composites can be processed into monoliths and thin films, allowing a broadening of their range of applications. The surrounding silica phase seems to hinder greater weight loss of the carbon nitride phase by avoiding sublimation of melamine during condensation.

Experimental section

Synthesis of porous carbon nitride and silica

Cyanamide (CA) and tetraethylorthosilicate (TEOS) are used as sources to produce carbon nitrides and silica. Initially, a certain amount of CA is dissolved in 0.01 N HCl (4 g) and ethanol (4 g) and the pH is adjusted to 2 with 1 N HCl solution followed by the addition of required amount of TEOS (x : y—1 : 3, 1 : 6, 1 : 12, x and y are molar ratios of TEOS : CA). The mixtures were stirred for 30 min and poured into Petri dishes. After evaporation of the solvents, transparent glassy films are observed, which were heated to 80 °C for 24 h. The resulting films were heated to 550 °C within 4 h in an argon atmosphere and heat treated at this temperature for further 4 h. To obtain pure silicas the resulting silica–carbon nitride composites are further heated to 650 °C for 5 h in ambient conditions and left at this temperature for 1 h. To obtain pure carbon nitride the composites are treated with 4 M NH_4HF_2 solution for 40 h and subsequent washing with water for several times and finally with ethanol.

Characterization

The X-ray diffraction (XRD) measurements were performed on a Bruker D8 Advance X-ray diffractometer using CuKα_1 irradiation ($\lambda = 0.154$ nm). Nitrogen sorption analyses were carried out on an Autosorb-1 instrument after evacuating the samples at 150 °C overnight. The surface areas are determined by applying the Brunauer–Emmett–Teller (BET) method in the relative pressure range of 0.05–0.25. The pore volume is calculated at the relative pressure of 0.99. The pore diameter and distribution are obtained by using the Barrett–Joyner–Halenda (BJH) method. The solid-state NMR $^{29}Si\{^1H\}$ and $^{13}C\{^1H\}$ CP/MAS (cross-polarization magic angle spinning) measurements were carried out using a Bruker Advance 400 spectrometer operating at 79.4 and 100.6 MHz for ^{29}Si and ^{13}C using a Bruker 4 mm double resonance probe-head operating at a spinning rate of 10 and 6 kHz, respectively. ^1H composite pulse decoupling was applied during the acquisition. ^{29}Si chemical shifts were determined relative to the external standard Q_8M_8, the trimethylsilyl ester of octameric silicate, and were then referenced to TMS. ^{13}C chemical shifts were referenced externally to TMS (tetramethylsilane) using adamantane as a secondary reference. Transmission electron microscope (TEM) images were obtained from a FEI Tecnai

Table 1 Porous features of the carbon nitride, silica and their composites[a]

Sample code	TEOS : CA	S_{BET}/m^2 g^{-1}	V_{tp}/cm^3 g^{-1}	V_{micro}/cm^3 g^{-1}	V_{meso}/cm^3 g^{-1}	D_p/nm
CN-SIL-3	1 : 3	270	0.31	0.03	0.28	5.6
CN-SIL-6	1 : 6	77	0.16	0.01	0.15	16.4
CN-SIL-12	1 : 12	6	0.01	—	0.01	—
CN-3	1 : 3	1	0.01	0.01	—	—
CN-6	1 : 6	131	0.16	0.05	0.11	2.4
CN-12	1 : 12	167	0.19	0.02	0.17	3.6
SIL-3	1 : 3	864	0.56	0.48	0.08	2.6
SIL-6	1 : 6	939	0.92	0.46	0.46	4.9
SIL-12	1 : 12	901	1.17	0.52	0.65	6.5

[a] CN-carbon nitride, SIL-silica, TEOS : CA-tetraethylorthosilicate : cyanamide molar ratio, S_{BET}-surface area, V_{tp}-total pore volume, V_{micro}-pore volume from micropores, V_{meso}-pore volume from mesopores, and D_p-pore diameter.

20 microscope, using carbon-coated copper grids. Elemental analysis was performed on a Vario Micro setup. TGA measurements were done on a PerkinElmer STA 6000 instrument in ambient conditions with the heating rate of 10 °C min^{-1}. UV-Visible measurement was carried out on a Cary 300 scan UV-Visible spectrophotometer in diffuse reflectance mode using barium sulfate as reference.

Photocatalytic tests

As a standard procedure a double walled, thermostatically controlled reaction vessel was evacuated and filled with argon six times to remove any other gas. First the carbon nitride and the cocatalyst K_2PtCl_6 were added in Teflon crucibles, then 20 mL of the solvent mixture H_2O/TEOA (triethanolamine) 9 : 1 were added and the temperature was maintained at 25 °C by a thermostat. After stirring for 5 min at that temperature the reaction was started by switching on the xenon light source with a 395 nm cut-off filter and a light output of 1.5 W cm^{-2}. The amount of formed hydrogen was monitored by means of an automatic gas burette and the gas mixture was analysed and quantified by GC as described elsewhere.[22] For recycling experiments the solvent was removed under an argon atmosphere and a freshly prepared solvent mixture was added to the reaction vessel for the next run.

Results and discussions

To prepare the composites, cyanamide and TEOS are mixed in an acidified water/ethanol solution. As cyanamide is a base, the pH has to be adjusted to the isoelectric point of silica (pH = 2) prior to addition of TEOS. After mixing a transparent homogeneous solution is formed showing the solubility of cyanamide and TEOS and subsequently formed silicic acid in water/ethanol. After pouring these solutions in Petri dishes and evaporation of the solvents under ambient conditions, colorless, transparent films are formed (Fig. S1†). The films stay transparent after tempering at 80 °C, which was carried out to facilitate further condensation of the silica phase. The formation of transparent films excludes the possibility of macrophase separation of the cyanamide from the silica phase. Thermal treatment of the hybrid materials to 550 °C was carried out to yield thermal condensation of the cyanamide to melamine, melem and finally a condensed carbon nitride.

The samples presented in this study are named as described in Table 1 (*e.g.* for the composition TEOS : CA—1 : 3, the obtained carbon nitride and silica are denoted as CN-3 and SIL-3, respectively and the composites as CN-SIL-3).

With increasing amount of cyanamide in the solutions a higher amount of carbon nitride in the resulting composites is observed, which was proven by thermogravimetric analysis (TGA) (Fig. S2†). The carbon nitride amount could be assessed to 18, 32, 53 wt% for the samples CN-3, CN-6 and CN-12 respectively. Assuming the weight losses of the precursors (TEOS → SiO_2, 3*x*CA → C_3N_4) it can be concluded that also in this approach, carbon nitride yields are low (calculated amounts for quantitative yields are 60, 75, 85 wt%). However it should be noted that the same approach with pure cyanamide (poured from a solvent on a Petri dish) would yield no product due to full sublimation of the intermediate melamine.

Two possible structures of the composite can be envisaged: first the formation of a homogenous phase of a covalently bound silicon–oxygen–carbon–nitrogen network or the formation of two separated silica/carbon nitride phases, which however just show microphase separation. A quite similar mechanism was found for the formation of phenol formaldehyde/silica and

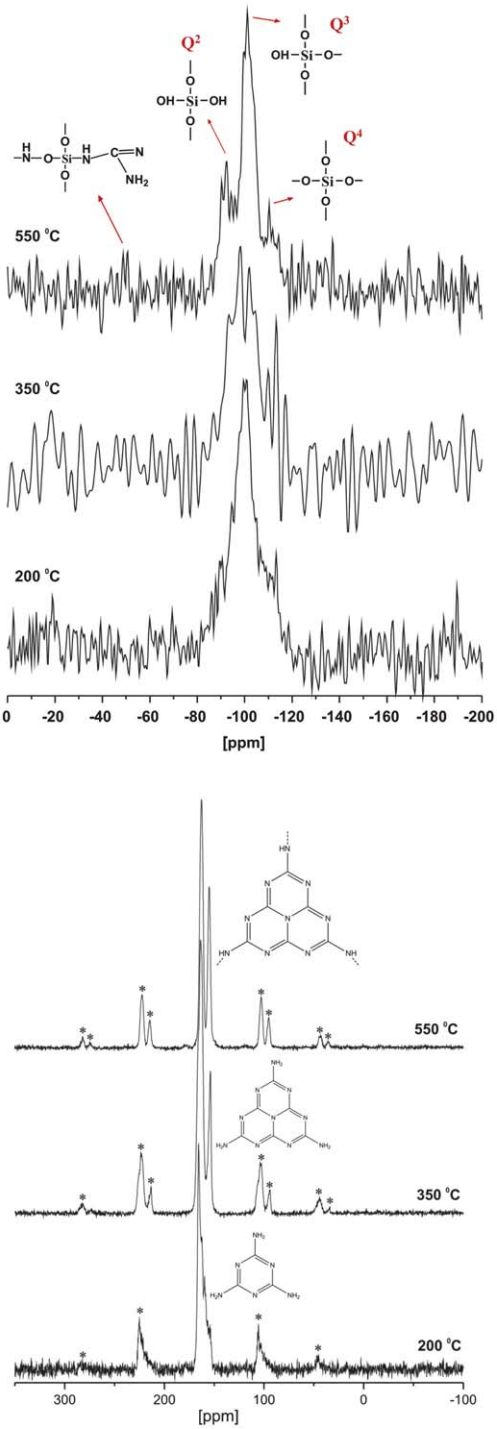

Fig. 1 Solid-state $^{29}Si\{^1H\}$ (top) and $^{13}C\{^1H\}$ CP/MAS NMR spectra (bottom) of the carbon nitride–silica composite, CN-SIL-12. * indicates the spinning side bands in the ^{13}C spectra.

carbon/silica composites, prepared by the co-assembly of polymer and silica precursors.[23]

To evaluate the microstructure of the composite solid-state $^{29}Si\{^1H\}$ and $^{13}C\{^1H\}$ CP/MAS NMR have been carried out on CN-SIL-12 (Fig. 1) heated to different temperatures. The ^{29}Si NMR spectra are quite similar to a pure silica phase prepared from TEOS and heated to the respective temperatures. Signals at around −110, −100 and −92 ppm indicate the different condensation degrees of the silica phase which corresponds to Q^4, Q^3 and Q^2 groups respectively. Just very weak signals attributable to covalent interactions between the silica and carbon nitride phases (for example by Si–N bonds located around −45 ppm) are observed from these measurements, which might be formed at the SiO_2/CN interface. ^{13}C NMR spectra for the sample heated at 200 °C show the formation of melamine with a signal at 166 ppm. The samples heated at 350 and 550 °C with signals at around 154 and 163 ppm show the formation of tri-*s*-triazine signals as can be expected for the formation of melem, melon and the final carbon nitride. Thus NMR spectra are observed which resemble the pure SiO_2 and CN phase, respectively, indicating that indeed two separate phases have been formed which interact mainly *via* hydrogen bonding and electrostatic interactions between the amine groups and the silanol groups. To verify this assumption, one of the two phases was selectively removed by either thermal treatment or HF etching.

Scheme 1 shows the assumed structure of the composite and the steps to obtain the pure silica and carbon nitride phase, respectively.

For such a microphase separated structure it can be assumed that after removal of the second phase a highly porous structure remains. This will however just hold true, when the materials are forming continuous, interpenetrating phases (Scheme 1).

The porous characteristics of the composites and pure carbon nitride and silica after removal of the second phase were analyzed by nitrogen physisorption measurements (Table 1).

Already the composites CN-SIL-3 and CN-SIL-6 are porous showing a type IV isotherm typical for mesoporous materials with surface areas of 270 and 77 $m^2\ g^{-1}$, respectively (Fig. S3†). During heat treatment it can be expected that the carbon nitride phase shrink to a larger extent than the silica phase, as the starting compound, cyanamide, is condensing into a more compact polymer under continuous evaporation of ammonia. The unequal shrinkage of the two phases explains the porosity observed already in the composites, as it can be assumed that the resulting carbon nitride does not fill the first formed silica voids completely. This effect is mainly observed for higher silica/CN ratios as a more stable and interconnected silica phase can be formed, while for lower amounts of silica (1 : 12) it seems that the silica phase follows the shrinkage of the forming carbon nitride, yielding in no porosity of the composites. The sorption measurements of the pure carbon nitride (Fig. 2a) and silica (Fig. 2c) after removal of the respective second phase show type IV isotherms for all materials (except CN-3, showing no porosity).

CN-12 shows the highest pore volume and surface area of all the carbon nitrides. An average pore diameter of 3.6 nm can be estimated from the BJH pore size distribution (Fig. 2b). CN-6 shows lower but still significant porosity and surface area with pore diameter centered at 2.4 nm. CN-3 finally shows no porosity. Thus against first expectations an increasing amount of silica yields decreasing porosity in the replica. This result shows the limits of templating approaches to prepare porous carbon nitrides, as a certain pore wall thickness is mandatory to observe stable mesoporous materials. Thinner pore walls first yield shrinkage of the pores and finally collapse as observed for CN-6 and CN-3, respectively. The average thickness of the carbon nitride phase in this composite can indeed be anticipated from the investigation of the pure silica phase. Here pores with average diameters of 2.6, 4.9 and 6.5 nm are observed with increasing cyanamide ratio, reflecting the dimensions of the carbon nitride phase.

The silicas obtained after the removal of the carbon nitride phase from all the three samples are porous with high surface areas and pore volumes (Table 1). It can be assumed that the amorphous silica replicates much better the structure of the composite than the less stable carbon nitride. Indeed, the average pore size and pore volume of the silica increase with increasing amount of the carbon nitride phase, that is, when higher CA/TEOS ratios are used (Fig. 2d).

Transmission electron microscopy (TEM) images (Fig. 3) of the carbon nitride and silica phases confirm the results from the nitrogen sorption measurements. Unordered but continuous pore structures are observed in all cases, except for CN-3 where no porosity is observed. The silica materials nicely reflect the biphasic structure of the composite. Lower amounts of CA and thus of carbon nitride in the composites yield a dense silica phase with small, rather defined pores (Fig. 3c), while at higher CA

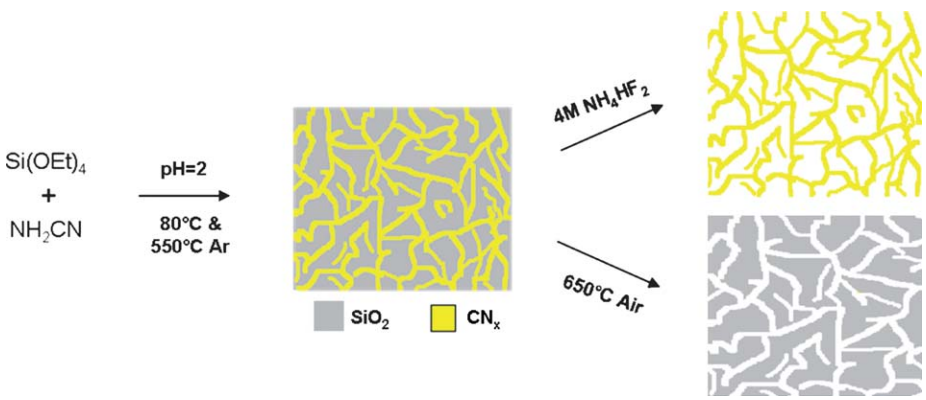

Scheme 1 The sol–gel route to obtain porous carbon nitride and silica.

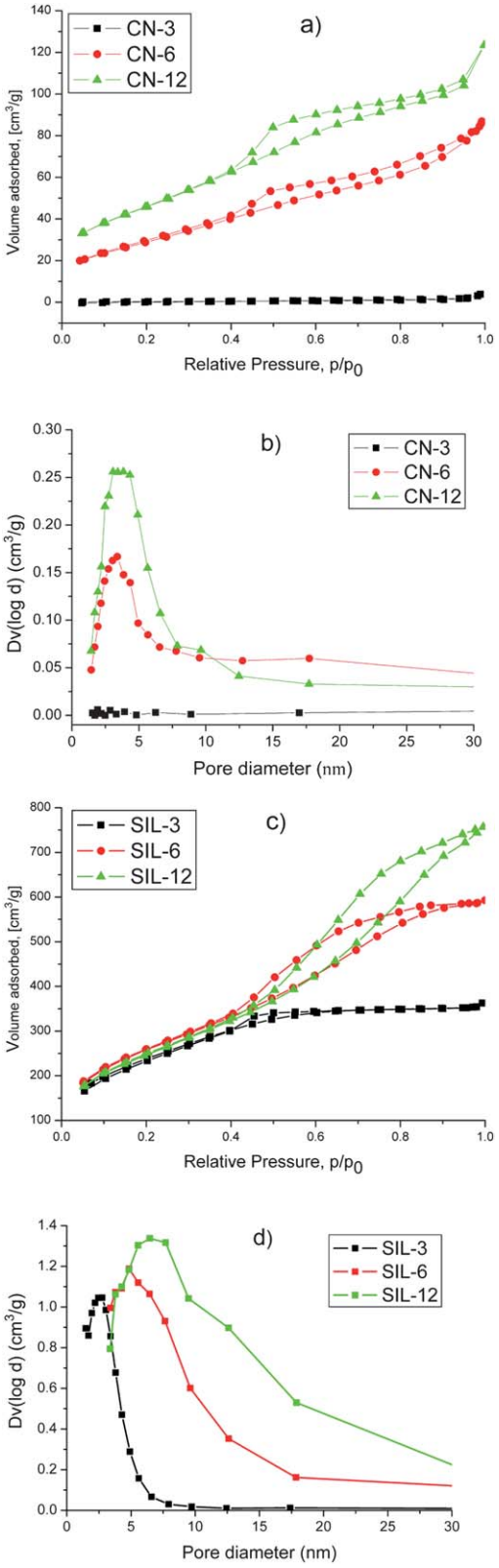

Fig. 2 Nitrogen sorption isotherms and pore size distribution of the carbon nitride (a and b) and silica materials (c and d), respectively.

concentrations, thinner silica pore walls can be seen (Fig. 3d and e). For the carbon nitride phase on the other hand higher CA amounts yield a more compact carbon nitride.

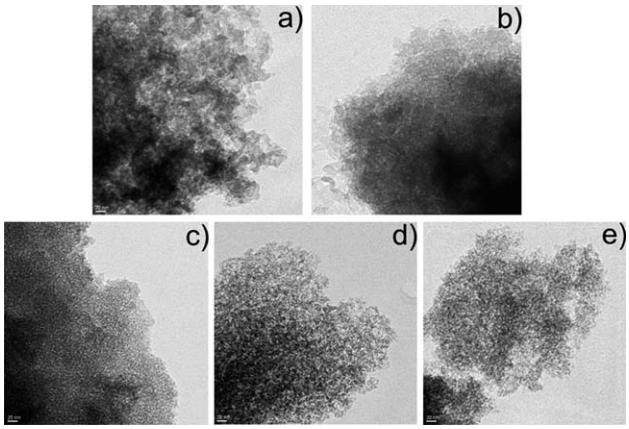

Fig. 3 TEM images of the carbon nitrides, (a) CN-6, (b) CN-12 and silicas, (c) SIL-3, (d) SIL-6 and (e) SIL-12 materials.

The carbon nitride phases were examined in more detail by elemental analysis, XRD and UV-Vis spectroscopy. Elemental analyses of the carbon nitrides gave a C/N ratio of 0.68, 0.70 and 0.67 for CN-3, CN-6 and CN-12, respectively. These values are in accordance with the C/N ratios of the bulk carbon nitride prepared by thermal condensation of cyanamide, while for an ideal graphitic carbon nitride a value of 0.75 is calculated (Table S1, ESI†). Also the materials still exhibit a considerable amount of hydrogen (~2 wt%) which points to incomplete condensation of the tri-*s*-triazine units.[4,5] In addition the high surface areas introduced in these materials generate multiple

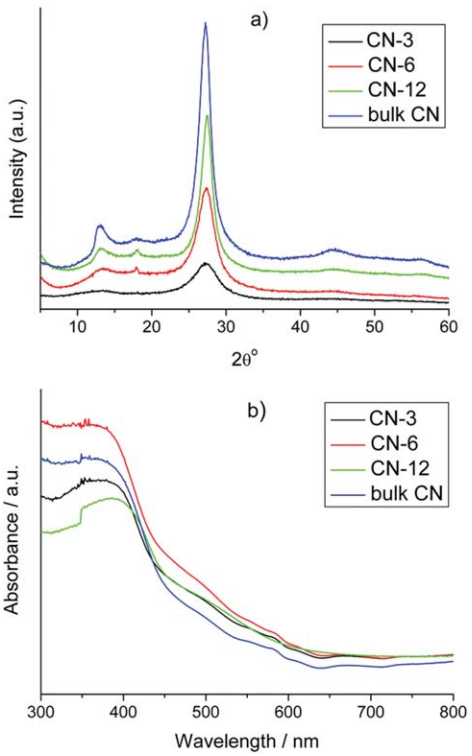

Fig. 4 Wide-angle powder XRD patterns (a) and UV-visible diffuse reflectance spectra (b) of the carbon nitride materials.

termination sites which increase the number of free amino groups and the amount of hydrogen in the structures.

The wide-angle X-ray diffraction patterns of all carbon nitride samples (Fig. 4a) reveal the graphite-like stacking of the carbon nitride layers, seen in the intense peak at 27.4°, corresponding to an interlayer distance of 0.326 nm (resembling the (002) reflection of graphite). When compared to the bulk carbon nitride sample, an overall decrease in intensity of the signal and peak broadening is observed from samples prepared with higher silica amount, thus thinner pore walls of the carbon nitride. This supports the assumption that lower CA contents yield a spatial confinement, which prevents the formation of extended graphitic layers. In the extreme case, the pore walls are too thin so that the pore structure of the carbon nitride collapses. This was also shown in an earlier study producing the 2D-hexagonal SBA-15 replica of the carbon nitride where smaller micropores are not able to incorporate the highly graphitic, 2D anisotropic crystalline structure of the carbon nitrides.[17] It should be noted that so far no carbon nitride material which possess graphitic stacking with such small mesopores (~3 nm) has been reported, while this has been achieved for amorphous carbon nitrides.[15,16]

The UV-Vis diffuse reflectance spectrum of the CN samples reveals a strong absorption in the visible region for all the samples (Fig. 4b). The absorbance of the carbon nitrides is similar to the one from bulk samples, in which the steep band at 450 nm corresponds to the band gap transitions from N2p to C2p orbitals typical of semiconductor type electron transition.[7] The shoulder band from 450 to 600 nm is most likely attributed to the presence of impurities such as carbon (*e.g.* doped in the CN structure from the occluded ethanol during the thermal condensation process), which enhances the optical absorption of CN materials. Similar observation was reported for carbon nitride with enhanced carbon content prepared by co-polymerisation or heteroatom doped carbon nitrides in which there is a significant extension of the spectrum in the visible range.[24,25]

The facile sol–gel route employed to prepare these materials allows processing the materials in different morphologies like thin films and monoliths. Fig. 5 shows a monolith obtained from the TEOS : CA—1 : 6 composition. A transparent glassy monolith was prepared pouring the precursor solution into a plastic mold and allowing the solvent to evaporate. After heat treatment (550 °C) the monolith has shrunk to some extent but overall stays in shape (Fig. 5). Further, the removal of silica with 4 M NH_4HF_2 solution results in a yellow monolith.

Photocatalytic activity of the resulting CN compounds for water reduction has been investigated using platinum as the water reduction catalyst and triethanolamine (TEOA) as the sacrificial reductant (Table 2 and Fig. S4†). Experiments 1–5 in Table 2 demonstrate that all components of this system are essential to produce hydrogen with light. Within the detection limits no hydrogen was detected in reactions without Pt and TEOA (entry 2, Table 2), with Pt but no TEOA (entry 4, Table 2) or with TEOA but no Pt (entry 3, Table 2). Only very low activity

Fig. 5 Monoliths of the carbon nitride/silica nanoporous composites.

Table 2 Photocatalytic investigation of CN compounds in the hydrogen evolution reaction from water. Light source: Xe-lamp (output 1.5 W cm^{-2}), 395 nm cut-off filter, 25 °C

Entry	Sample	Catalyst/ K_2PtCl_6/ mg	Water/ mL	Sacrificial reagent/ TEOA/ mL	H_2/mL[b]
1			20		2.1 (blank)[a]
2	12 mg CN-6		20		[a]
3	12 mg CN-6		18	2	[a]
4	12 mg CN-6	1.2	20		[a]
5	12 mg CN-6	1.4	18	2	21.5
6	50 mg mpg-C_3N_4[c]	5	18	2	25.5
7	50 mg CN-3	5	18	2	4.2
8	50 mg CN-6	5	18	2	40.5
9	50 mg CN-12	5	18	2	38

[a] No hydrogen detected within detection limits. [b] Hydrogen production within a 24h experiment (see Fig. S4†) [c] prepared according to reference [6].

was observed for CN-3 (4.2 mL in 24 h) which has no porosity and a marginal surface area. Samples CN-6 and CN-12 gave a much higher hydrogen yield of 40.5 mL and 38.0 mL in 24 h which is even higher than a reference mpg-C_3N_4 sample (prepared from Ludox HS 40 colloidal silica, 40 wt% suspension in water having surface area about 180 m^2 g^{-1})[6] with 25.5 mL under the same conditions.

These activities are against the expected trend when the surface area of the materials is compared. This shows again that high surface areas and porosities are obviously not the only prerequisites to reach high photocatalytic efficiencies with carbon nitride materials, but that a certain pore wall thickness is equally important.[9,26] Indeed, there are several effects of how nanostructuration in general, and the introduction of mesoporosity in particular, can influence the photocatalytic activity of a semiconducting material. On the one hand, introduction of small pores yields a larger amount of surface active sites accessible for incoming photons, water and sacrificial agents and also co-catalysts can better be dispersed. On the other hand, increasing the surface area is accompanied with thinning of the pore walls which can yield numerous defect sites, disturbing or even disrupting the conjugated structure of the carbon nitride which deteriorate its semiconducting properties. Also separation of electrons and holes might be inefficient in such smaller confinements represented by the thin pore walls. Studies to elucidate the effect of these different processes are currently under investigation.

CN-6 and CN-12 show a nearly linear reaction curve in a 24 h experiment (Fig. S4†). However, a decreased reaction rate was observed in a recycling experiment of CN-6 with and without addition of Pt after the separation of the solid components (Fig. S5 and S6†). Addition of fresh Pt thus does not lead to increased activity indicating that passivation of the carbon nitride surface is responsible for the deactivation. On the other hand in a long term (96 h) experiment, in which CN-6 also shows a slight decrease in activity (Fig. S7†), it was observed that the orange suspension turns to a more grayish one during this time. This on the other hand points to ripening of the Pt co-catalyst, which might thus also affect the activity of this photocatalyst in the long term.

Conclusions

A combined sol–gel/thermal condensation route is employed to synthesize interpenetrated mesostructures of carbon nitride and silicas. The precursors of these two compounds are mixed and condensed simultaneously yielding a biphasic silica/carbon nitride composite. Selective removal of one of the phases yields a mesoporous carbon nitride and silica, respectively. The porous characteristics of these phases can be tuned to obtain materials with different surface areas, pore volumes and pore sizes by simply adjusting the ratio of the starting precursors. Carbon nitrides with small mesopores (~3 nm) are synthesized preserving the graphitic stacking of the carbon nitride sheets. The sol–gel approach furthermore provides a facile pathway towards processing of mesoporous carbon nitrides exemplified by the formation of monoliths. The photocatalytic activity of the mesoporous carbon nitrides prepared by this approach is much higher than observed for bulk and even mesoporous carbon nitrides prepared using pre-formed silica templates.

We believe that the here presented sol–gel route is a first step towards the preparation of larger photoelectrodes based on mesoporous carbon nitrides. Work on the preparation of mesoporous carbon nitrides on electrodes and measurements of their photocatalytic performance is in progress. This approach can be further extended to the direct preparation of semiconductor nanocomposites based on carbon nitride/metal oxide systems by using other oxide sources than silica alkoxides.

Acknowledgements

This work was supported by the Project "Light2Hydrogen" of the BMBF (03IS2071D).

References

1 E. Kroke and M. Schwarz, *Coord. Chem. Rev.*, 2004, **248**, 493–532.
2 A. Thomas, A. Fischer, F. Goettmann, M. Antonietti, J.-O. Müller, R. Schlögl and J. M. Carlsson, *J. Mater. Chem.*, 2008, **18**, 4893–4908.
3 E. Kroke, M. Schwarz, E. Horath-Bordon, P. Kroll, B. Noll and A. D. Norman, *New J. Chem.*, 2002, **26**, 508–512.
4 B. V. Lotsch and W. Schnick, *Chem. Mater.*, 2006, **18**, 1891–1900.
5 B. V. Lotsch, M. Doeblinger, J. Sehnert, L. Seyfarth, J. Senker, O. Oeckler and W. Schnick, *Chem.–Eur. J.*, 2007, **13**, 4969–4980.
6 F. Goettmann, A. Fischer, M. Antonietti and A. Thomas, *Angew. Chem., Int. Ed.*, 2006, **45**, 4467–4471.
7 X. C. Wang, K. Maeda, A. Thomas, K. Takanabe, G. Xin, J. M. Carlsson, K. Domen and M. Antonietti, *Nat. Mater.*, 2009, **8**, 76–80.
8 K. Maeda, X. C. Wang, Y. Nishihara, D. Lu, M. Antonietti and K. Domen, *J. Phys. Chem. C*, 2009, **113**, 4940–4947.
9 X. C. Wang, K. Maeda, X. Chen, K. Takanabe, K. Domen, Y. Hou, X. Fu and M. Antonietti, *J. Am. Chem. Soc.*, 2009, **131**, 1680–1681.
10 X. Chen, Y.-S. Jun, K. Takanabe, K. Maeda, K. Domen, X. Fu, M. Antonietti and X. C. Wang, *Chem. Mater.*, 2009, **21**, 4093–4095.
11 A. Thomas, F. Goettmann and M. Antonietti, *Chem. Mater.*, 2008, **20**, 738–755.
12 A. Thomas, *Angew. Chem., Int. Ed.*, 2010, **49**, 8328.
13 Y. Wang, X. C. Wang, M. Antonietti and Y. Zhang, *ChemSusChem*, 2010, **3**, 435–439.
14 M. Groenewolt and M. Antonietti, *Adv. Mater.*, 2005, **17**, 1789–1792.
15 A. Vinu, K. Ariga, T. Mori, T. Nakanishi, S. Hishita, D. Golberg and Y. Bando, *Adv. Mater.*, 2005, **17**, 1648–1652.
16 L. Liu, D. Ma, H. Zheng, X. Li, M. Cheng and X. Bao, *Microporous Mesoporous Mater.*, 2008, **110**, 216–222.
17 Y.-S. Jun, W. H. Hong, M. Antonietti and A. Thomas, *Adv. Mater.*, 2009, **21**, 4270–4274.
18 E. Z. Lee, Y.-S. Jun, W. H. Hong, A. Thomas and M. M. Jin, *Angew. Chem., Int. Ed.*, 2010, **49**, 9706–9710.
19 C. Niu, Y. Z. Lu and C. M. Lieber, *Science*, 1993, **261**, 334–337.
20 L. P. Guo, Y. Chen, E. G. Wang, L. Li and Z. X. Zhao, *Chem. Phys. Lett.*, 1997, **268**, 26–30.
21 A. K. M. S. Chowdury, D. C. Cameron, M. S. J. Hashmi and J. M. Gregg, *J. Mater. Res.*, 1999, **14**, 2359–2363.
22 F. Gärtner, B. Sundararaju, A.-E. Surkus, A. Boddien, B. Loges, H. Junge, P. H. Dixneuf and M. Beller, *Angew. Chem., Int. Ed.*, 2009, **48**, 9962–9965.
23 R. Liu, Y. Shi, Y. Wan, Y. Meng, F. Zhang, D. Gu, Z. Chen, B. Tu and D. Zhao, *J. Am. Chem. Soc.*, 2006, **128**, 11652–11662.
24 J. Zhang, X. Chen, K. Takanabe, K. Maeda, K. Domen, J. D. Epping, X. Fu, M. Antonietti and X. C. Wang, *Angew. Chem., Int. Ed.*, 2010, **49**, 441–444.
25 J. Zhang, J. Sun, K. Maeda, K. Domen, P. Liu, M. Antonietti, X. Fu and X. C. Wang, *Energy Environ. Sci.*, 2011, **4**, 675–678.
26 A. Deshpande and N. M. Gupta, *Int. J. Hydrogen Energy*, 2010, **35**, 3287–3296.

